REFERENCES

Baldi, M., Finocchio, E., Milella, F. and Busa, G., "Catalytic combustion of C3 hydrocarbons and oxygenated over Mn_3O_4", *Appl. Catal B.*, 1998, **16**, 43-51.

Busca, G., Guidetti, R. and Lorenzelli, V., "Fourier-transform Infrared Study of the Surface Properties of Cobalt Oxides", *J. Chem. Soc., Faraday Trans.*,1990, **86**, 989-994.

Chaar, M. A., Kung, H. H. and Patel, D., "Selective Oxidative Dehydrogenation of Butane over V-Mg-O catalysts", *J. Catal.*, 1987, **105**, 483-498.

Chaar, M. A., Patel, D. and Kung, H. H., "Selective Oxidative Dehydrogenation of Propane over V-Mg-O Catalysts", *J. Catal.*, 1988, **109**, 463-467.

Chan, T. K. and Smith, K. J., "Oxidative Coupling of Methane over Cobalt-Magnesium and Manganese-Magnesium Mixed Oxide Catalysts", *Appl. Catal.*, 1990, **60**, 13-31.

Corma, A., Nieto, J. M. L. and Paredes, N., "Preparation of V-Mg-O catalysts: Nature of active species precusors", *Appl. Catal.*, 1993, **104**, 161-174.

Corma, A., Nieto, J. M. L. and Paredes, N., "Influence of the Preparation Methods Of V-Mg-O catalysts on Their Catalytic Properties for the Oxidative Dehydrogenation of Propane", *J. Catal.*, 1993, **144**, 425-435.

Drago, R., Jurczyk, K. and Kob, N., "Catalyzed decomposition of N_2O on metal oxide supports", *Appl. Catal B.*, 1997,**13**, 69-79.

Finocchio, E., Willey, R. J., Busca, G. and Lorenzelli, V., "FTIR studies on the selective oxidation and combustion of light hydrocarbons at metal oxide surfaces", *J. Chem. Soc.,Faraday Trans.*,1997, **93**, 175-180.

Gao,X., Ruiz, P., Xin, Q., Guo, X. and Delmon, B., "Preparation and characterization of three pure magnesium vanadate phases as catalysts for selective oxidation of propane to propene", *Catal. Lett.*, 1994, **23**, 321-337.

Garbowski, E., Guenin, M., Marion, M-C. and Primet, M., "Catalytic Properties and Surface States of Cobalt Containing Oxidation Catalysts", *Appl. Catal.*, 1990, **64**, 209-224.

Grabowski, R., Grzybowska, B., Samson, K., Sloczynski, J., Stoch, J. and Wcislo, K., "Effect of Alkaline Promoters on Catalytic Activity of V_2O_5/TiO_2 and MoO_3/TiO_2 catalysts in Oxidative Dehydrogenation of Propane and in Isopropanol Decomposition", 1995, *Appl. Catal.*, **125**, 129-135.

Grabowski, R., Grzybowska, B., Sloczynski, J and Wcislo, K., "Oxidative dehydrogenation of isobutane on supported chromia catalysts", *Appl. Catal.*, 1996, **144**, 335-341.

Grzybowska, B., Sloczynski, J., Grabowski, R., Wscilo, K., Kozlowska, A., Stoch, J. and Zielinski, J., "Chromium Oxide/Alumina Catalysts in Oxidative Dehydrogenation of Isobutane", *J. Catal.*, 1998, **178**, 687-700.

Halawy, S. A. and Mohamed, M. A., "Characterization of Unsupported Molybdenum Oxide-Cobalt Oxide Catalysts", *J. Chem. Tech. Biotechnol.*, 1993, **58**, 237-245.

Hilmen, A. M., Schanke, D. and Holmen, A., "TPR study of the mechanism of rhenium promotion of alumina-supported cobalt Fisher-Tropsch catalysts", *Cat. Lett.*, 1996, **38**, 143-147.

Kang, Y-M. and Wan, B-Z., "Effects of acid or base additives on the catalytic combustion activity of Chromium and Cobalt oxides", *Appl. Catal A.*, 1994, **114**, 35-49.

Luo, M-f., Yuan, X-x. and Zheng, X-m., "Catalyst characterization and activity of Ag-Mn, Ag-Co and Ag-Ce composite oxides for oxidation of volatile organic compounds", *Appl. Cat.*, 1998, **175**, 121-129.

Mars, P. and van Krevelen, D. W., "Oxidations carried out by means of vanadium oxide catalysts", *Chem. Eng. Sc.*, 1954, **3**, 41-59.

Okamoto, Y., Adachi, T., Nagata, K., Odawara, M. and Imanaka, T., "Effects of Starting cobalt salt upon the cobalt-alumina interactions and hydrodesulfurization activity of CoO/Al_2O_3", *Appl. Catal.*, 1991, **73**, 249-265.

Pepe, F. and Occhiuzzi, M., "Surface Characterization and Catalytic Activity of $Co_xMg_{1-x}AL_2O_4$ Solid Solution", *J. Chem. Soc., Faraday Trans.*, 1994, **90**, 905-910.

Perry, R. H. and Chilton, C. H., *Chemical Engineering*, Handbook, 1973, Fifth Edition.

Reid, R. C., Prausnitz, J. M., and Poling, B.E., *The properties of Gases & Liquids*, McGraw-Hill Company, 1988, Fourth Edition.

Sam, K., Soenen, V. and Volta, J. C., "Oxidative Dehydrogenation of Propane over V-Mg-O catalysts", *J. Catal.*, 1990, **123**, 417-435.

Santos, A., Menendez, M., Monzon, A.,Santamaria, J.,Miro, E. E.and Lombardo, E.A., "Oxidation of Methane to Synthesis Gas in Fluidized Bed Reactor Using MgO-Based Catalysts", *J. Catal.*, 1996, **158**, 83-91.

Satterfield, C. N., Heterogenous., " Catalytic Oxidation", *Heterogeneous Catalysis in Industrial Practice*, McGraw-Hill, 1991, Second Edition, 180-192.

Sinha, A. S. K. and Shankar, V., "Low-Temperature Catalysts for Total Oxidation of n-Hexane", *Ind. Eng. Chem. Res.*, 1993, **32**, 1061-1065.

Smith, J. M., *Chemical Engineering Kinetics*, McGreaw-Hill Book Company, 1981, Third edition.

Thammanokul, H., *Master of Engineering thesis Chulalongkorn University*, 1996.

Wang, W.-J. and Chen Y.-W., "Influence of metal loading on the reducibility and hydrogenation activity of cobalt/alumina catalysts", *Appl. Catal.*, 1991, 77, 223-233.

Yoon, Y.-S., Ueda, W. and Moro-oka., "Oxidative dehydrogenation of propane over magnesium molybdate catalysts", *Cat. Lett.*, 1995, **35**, 57-64 (a).

Yoon, Y.-S., Fujikawa, N., Ueda, W., Moro-oka, Y. and Lee, K.-W., "Propane Oxidation over various metal molybdate catalysts", *Catalysis Today*, 1995, **24**, 327-333 (b).

APPENDIX A
CALCULATION OF CATALYST PREPARATION

Preparation of 4Co-Mg-O, 8Co-Mg-O, and 12Co-Mg-O catalysts by the Wet Impregnation Method are shown as follow:

Reagent: - Cobalt acetate tetrahydrate [$Co(CH_3COO)_2 .4H_2O$]
Molecular weight = 249 g.

Suppport: - Magnesium oxide [MgO]
Molecular weight = 39 g.

Calculation for the preparation of the Co-Mg-O catalyst.

1) 4Co-Mg-O catalyst

The 4Co-Mg-O aqueous solution used in catalyst preparation consists of Co 4 wt.% and MgO 96 wt %. The amount of cobalt in 4Co-Mg-O catalyst is calculated as follows :

Basis: MgO 1 g.

If the weight of catalyst was 100 gram, 4C-Mg-O would compose of cobalt 4 g. and MgO 96 g. Therefore, in this system,

the amount of Co $= 4/96 \times 1$
$= 0.0417$ g.

Cobalt (Co) 0.0417 g was prepared from $Co(CH_3COO)_2 .4H_2O$ 99% then

the $Co(CH_3COO)_2 .4H_2O$ content $= (249 \times 0.0417 \times 100) / (59 \times 99)$
$= 0.178$ g.

2) 8Co-Mg-O catalyst

The 8Co-Mg-O aqueous solution used in catalyst preparation consists of Co 8 wt.% and MgO 92 wt %. The amount of cobalt in 8Co-Mg-O catalyst is calculated as follows :

Basis: MgO 1 g.

If the weight of catalyst was 100 gram, 8C-Mg-O would compose of cobalt 8 g. and MgO 92 g. Therefore, in this system,

the amount of Co $= 8/92 \times 1$

$= 0.08695$ g.

Cobalt (Co) 0.08695 g was prepared from $Co(CH_3COO)_2 .4H_2O$ 99% then

the $Co(CH_3COO)_2 .4H_2O$ content $= (249 \times 0.08695 \times 100) / (59 \times 99)$

$= 0.3712$ g.

3) 12Co-Mg-O catalyst

The 12Co-Mg-O aqueous solution used in catalyst preparation consists of Co 12 wt.% and MgO 88 wt %. The amount of cobalt in 12Co-Mg-O catalyst is calculated as follows :

Basis: MgO 1 g.

If the weight of catalyst was 100 gram, 12C-Mg-O would compose of cobalt 12 g. and MgO 88 g. Therefore, in this system,

the amount of Co $= 12/88 \times 1$

$= 0.1363$ g.

Cobalt (Co) 0.1363 g was prepared from $Co(CH_3COO)_2 .4H_2O$ 99% then

the $Co(CH_3COO)_2 .4H_2O$ content $= (249 \times 0.1363 \times 100) / (59 \times 99)$

$= 0.5819$ g.

APPENDIX B
CALCULATION OF DIFFUSIONAL LIMITATION EFFECT

In the present work there is doubt whether the external and internal diffusion limitations interfere with the 1-propanol reaction. Hence, the kinetic parameters were calculated based on the experimental data so as to prove the controlled system. The calculation is categorized into two parts; one of which is the external diffusion limitation, and the other is the internal diffusion limitation.

1. External diffusion limitation

The 1-propanol oxidation is considered to be an irreversible first order reaction occurred on the interior pore surface of catalyst particles in a fixed bed reactor. Assume isothermal operation for the reaction.

In the experiment, 4% 1-propanol in air was used as the unique reactant in the system. Molecular weight of air and 1-propanol are 29 and 60, respectively. Thus, the average molecular weight of the gas mixture was calculated as follows:

M_{AB} = $0.04\times60 + 0.96\times0.29$

= 30.24 g/mol

Calculation of reactant gas density

Consider the 1-propanol oxidation is operated at low pressure and high temperature. We assume that the gases are respect to ideal gas law. The density of such gas mixture reactant at various temperatures is calculated in the following.

$$\rho = \frac{PM}{RT} = \frac{1.0\times10^{5}\times30.24\times10^{-3}}{8.314T}$$

We obtained : $\rho = 0.779$ kg/m^3 at T = 200°C

$\rho = 0.705$ kg/m^3 at T = 250°C

$\rho = 0.643$ kg/m^3 at T = 300°C

$\rho = 0.592$ kg/m^3 at T = 350°C

Calculation of the gas mixture viscosity

The simplified methods for determining the viscosity of low pressure binary are described anywhere (Reid, 1988). The method of Wilke is chosen to estimate the gas mixture viscosity.

For a binary system of species 1 and species 2,

$$\mu_m = \frac{y_1 \mu_1}{y_1 + y_2 \Phi_{12}} + \frac{y_2 \mu_2}{y_2 + y_1 \Phi_{21}}$$

where μ_m = viscosity of the mixture

μ_1, μ_2 = pure component viscosity

y_1, y_2 = mole fractions

$$\phi_{12} = \frac{\left[1 + \left(\frac{\mu_1}{\mu_2}\right)^{1/2} \left(\frac{M_2}{M_1}\right)^{1/4}\right]^2}{\left[8\left(1 + \frac{M_1}{M_2}\right)\right]^{1/2}}$$

$$\phi_{21} = \phi_{12} \left(\frac{\mu_2}{\mu_1}\right)\left(\frac{M_1}{M_2}\right)$$

M_1, M_2 = molecular weight

Let 1 refer to 1-propanol and 2 to air

$M_1 = 60$ and $M_2 = 29$

The viscosity of pure 1-propanol at 200°C, 250°C, 300°C and 350°C are 0.0124, 0.0135, 0.015 and 0.0162 cP, respectively. The viscosity of pure air at 200°C, 250°C, 300°C and 350°C are 0.0248,0.0265,0.0285 and 0.030 cP, respectively [Perry (1973)].

At 200°C :

$$\phi_{12} = \frac{\left[1+\left(\frac{0.0124}{0.0248}\right)^{1/2}\left(\frac{29}{60}\right)^{1/4}\right]^2}{\left[8\left(1+\frac{60}{29}\right)\right]^{1/2}} = 0.510$$

$$\phi_{21} = 0.510\left(\frac{0.0248}{0.0124}\right)\left(\frac{60}{29}\right) = 2.110$$

$$\mu_m = \frac{0.04\times 0.0124}{0.04+0.96\times 0.510} + \frac{0.96\times 0.0248}{0.96+0.04\times 2.110} = 0.0237cP = 2.37\times 10^{-5}\, kg/m-\text{sec}$$

At 250°C :

$$\phi_{12} = \frac{\left[1+\left(\frac{0.0135}{0.0265}\right)^{1/2}\left(\frac{29}{60}\right)^{1/4}\right]^2}{\left[8\left(1+\frac{60}{29}\right)\right]^{1/2}} = 0.514$$

$$\phi_{21} = 0.514\left(\frac{0.0265}{0.0135}\right)\left(\frac{60}{29}\right) = 2.086$$

$$\mu_m = \frac{0.04 \times 0.0135}{0.04 + 0.96 \times 0.514} + \frac{0.96 \times 0.0265}{0.96 + 0.04 \times 2.086} = 0.2.54cP = 2.540 \times 10^{-5} kg/m - \text{sec}$$

At 300°C :

$$\phi_{12} = \frac{\left[1 + \left(\frac{0.015}{0.0265}\right)^{1/2} \left(\frac{29}{60}\right)^{1/4}\right]^2}{\left[8\left(1 + \frac{60}{29}\right)\right]^{1/2}} = 0.52$$

$$\phi_{21} = 0.52\left(\frac{0.0265}{0.015}\right)\left(\frac{60}{29}\right) = 2.043$$

$$\mu_m = \frac{0.04 \times 0.015}{0.04 + 0.96 \times 0.52} + \frac{0.96 \times 0.0265}{0.96 + 0.04 \times 2.043} = 0.0274cP = 2.740^{-5} kg/m - \text{sec}$$

At 350°C :

$$\phi_{12} = \frac{\left[1 + \left(\frac{0.0162}{0.030}\right)^{1/2} \left(\frac{29}{60}\right)^{1/4}\right]^2}{\left[8\left(1 + \frac{60}{29}\right)\right]^{1/2}} = 0.525$$

$$\phi_{21} = 0.525\left(\frac{0.030}{0.0162}\right)\left(\frac{60}{29}\right) = 2.011$$

$$\mu_m = \frac{0.04 \times 0.0162}{0.04 + 0.96 \times 0.525} + \frac{0.96 \times 0.030}{0.96 + 0.04 \times 2.011} = 0.0288cP = 2.88 \times 10^{-5} kg/m - \text{sec}$$

Calculation of diffusion coefficients

Diffusion coefficients for binary gas system at low pressure calculated by empirical correlation are proposed by Reid (1988). Wilke and Lee method is chosen

to estimate the value of D_{AB} due to the general and reliable method. The empirical correlation is

$$D_{AB} = \frac{\left(3.03 - \frac{0.98}{M_{AB}^{1/2}}\right)(10^{-3})T^{3/2}}{PM_{AB}^{1/2}\sigma_{AB}^{2}\Omega_{D}}$$

where D_{AB} = binary diffusion coefficient, cm^2/s

T = temperature, K

M_A, M_B = molecular weights of A and B, g/mol

$$M_{AB} = 2\left[\left(\frac{1}{M_A}\right)+\left(\frac{1}{M_B}\right)\right]^{-1}$$

P = pressure, bar

σ = characteristic length, ^0A

Ω_D = diffusion collision integral, dimensionless

The characteristic Lennard-Jones energy and Length, ε and σ, of nitrogen and propane are as follows: (Reid, 1988)

For C_3H_7OH : $\sigma(C_3H_7OH) = 4.549\ ^0A$, $\varepsilon/k = 576.7$

For air : σ (air) $= 3.711\ ^0A$, $\varepsilon/k = 78.6$

The simple rules are usually employed.

$$\sigma_{AB} = \frac{\sigma_A + \sigma_B}{2} = \frac{4.549 + 3.711}{2} = 4.13$$

$$\varepsilon_{AB}/k = \left(\frac{\varepsilon_A \varepsilon_B}{k^2}\right)^{1/2} = (576.7 \times 78.6)^{1/2} = 212.9$$

Ω_D is tabulated as a function of kT/ε for the Lennard-Jones potential. The accurate relation is

$$\Omega_D = \frac{A}{(T^*)^B} + \frac{C}{\exp(DT^*)} + \frac{E}{\exp(FT^*)} + \frac{G}{\exp(HT^*)}$$

where $T^* = \frac{kT}{\varepsilon_{AB}}$, A = 1.06036 , B = 0.15610 , C = 0.19300 , D = 0.47635 , E = 1.03587 , F = 1.52996 , G = 1.76474 , H = 3.89411

Then $T^* = \frac{473}{212.9} = 2.222$ at 200°C

$T^* = \frac{523}{212.9} = 2.456$ at 200°C

$T^* = \frac{573}{212.9} = 2.691$ at 200°C

$T^* = \frac{623}{212.9} = 2.926$ at 200°C

$$\Omega_D = \frac{1.06036}{(T^*)^{0.15610}} + \frac{0.19300}{\exp(0.47635T^*)} + \frac{1.03587}{\exp(1.529967^*)} + \frac{1.76474}{\exp(3.89411T^*)}$$

Ω_D = 1.038 ; 200°C

Ω_D = 1.006 ; 250°C

Ω_D = 0.979 ; 300°C

Ω_D = 0.956 ; 350°C

With Equation of D_{AB},

$$\text{At 200°C : } D(C_3H_7OH\text{-air}) = \frac{\left(3.03 - \frac{0.98}{30.24^{0.5}}\right)(10^{-3})473^{3/2}}{1 \times 30.24^{0.5} \times 4.13^2 \times 1.038}$$

$$= 3.01 \times 10^{-5} \quad m^2/s$$

$$\text{At } 250^{\circ}\text{C} : D(C_3H_7OH\text{-air}) = \frac{\left(3.03-\frac{0.98}{30.24^{0.5}}\right)(10^{-3})523^{3/2}}{1\times30.24^{0.5}\times4.13^{2}\times1.006}$$

$$= 3.62\times10^{-5} \quad m^2/s$$

$$\text{At } 300^{\circ}\text{C} : D(C_3H_7OH\text{-air}) = \frac{\left(3.03-\frac{0.98}{30.24^{0.5}}\right)(10^{-3})573^{3/2}}{1\times30.24^{0.5}\times4.13^{2}\times0.979}$$

$$= 4.26\times10^{-5} \quad m^2/s$$

$$\text{At } 350^{\circ}\text{C} : D(C_3H_7OH\text{-air}) = \frac{\left(3.03-\frac{0.98}{30.24^{0.5}}\right)(10^{-3})623^{3/2}}{1\times30.24^{0.5}\times4.13^{2}\times0.956}$$

$$= 5.04\times10^{-5} \quad m^2/s$$

Reactant gas mixture was supplied at 100 ml/min. in tubular microreactor used in the 1-propanol oxidation system at 30°C

1-propanol flow rate through reactor = 100 ml/min. at 30°C

The density of 1-propanol, $\rho = \frac{1.0\times10^{5}\times30.24\times10^{-3}}{8.314(273+30)} = 1.216\,kg/s$

Mass flow rate = $1.216\left(\frac{100\times10^{-6}}{60}\right) = 2.03\times10^{-6}$ kg/s

Diameter of quartz tube reactor = 6 mm

Cross-sectional area of tube reactor = $\frac{\pi(6\times10^{-3})^{2}}{4} = 2.83\times10^{-5}$ m^2

Mass Velocity, $G = \frac{2.03\times10^{-6}}{2.83\times10^{-5}} = 0.072$ kg/m^2-s

Catalysis size = 100-150 mesh = 0.178-0.126 mm

Average catalysis = (0.126+0.178)/2 = 0.152 mm

Find Reynolds number, Re_p, which is well known as follows :

$$Re_p = \frac{d_p G}{\mu}$$

We obtained

$$\text{At } 200^{\circ}\text{C} : \text{Re}_p = \frac{(0.152\times10^{-3}\times0.072)}{2.37\times10^{-5}} = 0.459$$

$$\text{At } 250^{\circ}\text{C} : \text{Re}_p = \frac{(0.152\times10^{-3}\times0.072)}{2.54\times10^{-5}} = 0.429$$

$$\text{At } 300^{\circ}\text{C} : \text{Re}_p = \frac{(0.152\times10^{-3}\times0.072)}{2.74\times10^{-5}} = 0.398$$

$$\text{At } 350^{\circ}\text{C} : \text{Re}_p = \frac{(0.152\times10^{-3}\times0.072)}{3.0\times10^{-5}} = 0.377$$

Average transport coefficient between the bulk stream and particles surface could be correlated in terms of dimensionless groups which characterize the flow conditions. For mass transfer the Sherwood number, $k_m\rho/G$, is an empirical function of the Reynolds number, d_pG/μ , and the Schmit number , $\mu/\rho D$. The j-factors are defined as the following functions of the Schmidt number and Sherwood numbers:

$$j_D = \frac{k_m\rho}{G}\left(\frac{a_m}{a_t}\right)(\mu/\rho D)^{2/3}$$

The ratio (a_m/a_t) allows for the possibility that the effective mass-transfer area a_m, may be less than the total external area, a_t, of the particles. For Reynolds number greater than 10, the following relationship between j_D and the Reynolds number well represents available data.

$$j_D = \frac{0.458}{\varepsilon_B}\left(\frac{d_pG}{\mu}\right)^{-0.407}$$

where G = mass velocity(superficial) based upon cross-sectional area of empty reactor ($G = u\rho$)

d_p = diameter of catalyst particle for spheres

μ = viscosity of fluid

ρ = density of fluid

ε_B = void fraction of the interparticle space (void fraction of the bed)

D = molecular diffusivity of component being transferred

Assume $\varepsilon_B = 0.5$

At 200°C ; $j_D = \frac{0.458}{0.5}(0.459)^{-0.407} = 1.257$

At 250°C ; $j_D = \frac{0.458}{0.5}(0.429)^{-0.407} = 1.292$

At 300°C ; $j_D = \frac{0.458}{0.5}(0.398)^{-0.407} = 1.333$

At 350°C ; $j_D = \frac{0.458}{0.5}(0.377)^{-0.407} = 1.362$

A variation of the fixed bed reactor is an assembly of screens or gauze of catalytic solid over which the reacting fluid flows. Their correlation is of the form

$$j_D = \frac{\varepsilon k_m \rho}{G}(\mu / \rho D)^{2/3}$$

Where ε is the porosity of the single screen.

Hence, $k_m = \left(\frac{j_D G}{\mu}\right)(\mu / \rho D)^{-2/3}$

$$k_m = \left(\frac{0.458G}{\varepsilon_B \rho}\right) Re^{-0.407} Sc^{-2/3}$$

Find k_m : At 200°C, $k_m = \left(\frac{1.257 \times 0.072}{0.779}\right)(0.541)^{-2/3} = 0.174$ m/s

At 250°C, $k_m = \left(\frac{1.292 \times 0.072}{0.705}\right)(0.601)^{-2/3} = 0.185$ m/s

At 300°C, $k_m = \left(\frac{1.333 \times 0.072}{0.643}\right)(0.663)^{-2/3} = 0.194$ m/s

$$\text{At } 350^{\circ}\text{C},\ k_m = \left(\frac{1.362\times 0.072}{0.592}\right)(0.723)^{-2/3} = 0.205 \text{ m/s}$$

Find Schmidt number, Sc : $Sc = \frac{\mu}{\rho D}$

$$\text{At } 200^{\circ}\text{C} : Sc = \frac{2.37\times 10^{-5}}{0.779\times 3.01\times 10^{-5}} = 0.541$$

$$\text{At } 250^{\circ}\text{C} : Sc = \frac{2.54\times 10^{-5}}{0.705\times 3.62\times 10^{-5}} = 0.601$$

$$\text{At } 300^{\circ}\text{C} : Sc = \frac{2.74\times 10^{-5}}{0.643\times 4.26\times 10^{-5}} = 0.663$$

$$\text{At } 350^{\circ}\text{C} : Sc = \frac{2.89\times 10^{-5}}{0.592\times 5.04\times 10^{-5}} = 0.723$$

Properties of catalyst

Density = 0.375 g/ml catalyst

Diameter of 100-150 mesh catalyst particle = 0.152 mm

$$\text{Weight per catalyst particle} = \frac{\pi(0.152\times 10^{-1})^3\times 0.375}{6} = 6.895\times 10^{-7} \text{ g/particle}$$

$$\text{External surface area per particle} = \pi(0.152\times 10^{-3})^2 = 7.26\times 10^{-8} \text{ m}^2\text{/particle}$$

$$a_m = \frac{7.260\times 10^{-8}}{6.895\times 10^{-7}} = 1.052\times 10^{-1} \text{ m}^2\text{/gram catalyst}$$

Volumetric flow rate of gaseous feed stream = 100 ml/min

1-Propanol molar feed rate = $0.04\times 6.62\times 10^{-5} = 2.65\times 10^{-6}$ mol/s

The estimated rate of 1-propanol oxidation reaction is based on the ideal plug-flow reactor which there is no mixing in the direction of flow and complete mixing perpendicular to the direction of flow (i.e., in the radial direction). The rate of reaction will vary with reaction length (L). Plug flow reactors are normally operated at steady state so that properties at any position are constant with respect to time. The mass balance around plug flow reactor becomes

For 1-propanol oxidation on 4Co-Mg-O catalyst, conversion (x) is 0.55 at 300°C.

$$\left\{\begin{matrix}\text{rate of i into}\\ \text{volume element}\end{matrix}\right\} - \left\{\begin{matrix}\text{rate of i out of}\\ \text{volume element}\end{matrix}\right\} + \left\{\begin{matrix}\text{rate of production of i within}\\ \text{the volume element}\end{matrix}\right\}$$
$$= \left\{\begin{matrix}\text{rate of accumulation of i within}\\ \text{the volume element}\end{matrix}\right\}$$

$$F_{AO} = F_{AO}(1 - x) + (r_w W)$$
$$(r_w W) = F_{AO} - F_{AO}(1 - x) = F_{AO}\, x$$
$$\text{At } 300\,^{o}C,\ r_w = \frac{F_{AO}\, x}{W} = \frac{2.65 \times 10^{-6} \times 0.55}{0.1} = 1.457 \times 10^{-5} \text{ mol/s - gram catalyst}$$

At steady state the external transport rate may be written in terms of the diffusion rate from the bulk gas to the surface. The expression is:

$$r_{obs} = k_m a_m (C_b - C_s)$$
$$= \frac{\text{1 - Propanol converted (mole)}}{\text{(time) (gram of catayst)}}$$

where C_b and C_s are the concentrations in the bulk gas and at the surface, respectively.

$$\text{At } 300^{\circ}\text{C},\ (C_b - C_s) = \frac{r_{obs}}{k_m a_m} = \frac{1.457 \times 10^{-5}}{0.194 \times 1.05 \times 10^{-1}} = 7.15 \times 10^{-4} \text{ mol/m}^3$$

At 200°, x = 0.20, $r_{obs} = 5.30 \times 10^{-6}$ mol/ s.cat, $C_b - C_s = 2.90 \times 10^{-4}$ mol/m^3

At 250°, x = 0.39, $r_{obs} = 1.03 \times 10^{-5}$ mol/ s.cat, $C_b - C_s = 5.30 \times 10^{-4}$ mol/m^3

At 300°, x = 0.55, r_{obs} = 1.45 × 10^{-5} mol/ s.cat, C_b-C_s = 7.15 × 10^{-4} mol/m^3
From C_b (propane) = 1.59 mol/m^3

Consider the difference of the bulk and surface concentration is small. It means that the external mass transport has no effect on the 1-propanol oxidation reaction rate.

2. Internal diffusion limitation

Next, consider the internal diffusional limitation of the 1-propanol oxidation reaction. An effectiveness factor, η, was defined in order to express the rate of reaction for the whole catalyst pellet, r_p, in terms of the temperature and concentrations existing at the outer surface (Smith, 1981) as follows:

$$\eta = \frac{\text{actual rate of whole pellet}}{\text{rate evaluated at outer surface conditions}} = \frac{r_p}{r_s}$$

The equation for the local rate (per unit mass of catalyst) may be expressed functionally as

$$r = f(C,T)$$

where C represents, symbolically, the concentrations of all the involved components. Then

$$r_p = \eta r_s = \eta f(C_s, T_s)$$

Suppose that the 1-propanol oxidation is an irreversible reaction A→B and first order reaction, so that for isothermal conditions $r = f(C_A) = k_1 C_A$. Then $r_p = \eta k_1 (C_A)_s$

For a spherical pellet, a mass balance over the spherical-shell volume of thickness Δr. At steady state the rate of diffusion into the element less the rate of

diffusion out will equal the rate of disappearance of reactant with in the element. This rate will be $\rho_p k_1 C_A$ per unit volume, where ρ_p is the density of the pellet. Hence, the balance may be written, omitting subscript A on C,

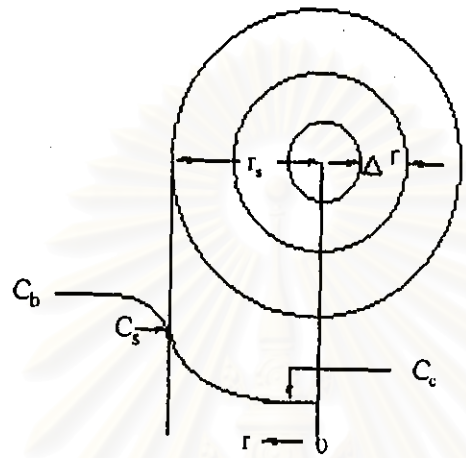

Figure B1 Reactant (A) concentration vs. position for first-order reaction on a spherical catalyst pellet.

$$\left(-4\pi r^2 De\frac{dC}{dr}\right)_r - \left(-4\pi r^2 De\frac{dC}{dr}\right)_{r+\Delta r} = -4\pi r^2 \Delta r \rho_p k_1 C$$

Take the limit as $\Delta r \rightarrow 0$ and assume that the effective diffusivity is independent of the concentration of reactant, this difference equation becomes

$$\frac{d^2C}{dr^2} + \frac{2dC}{rdr} - \frac{k_1 \rho_p C}{D_e} = 0$$

At the center of the pellet symmetry requires

$$\frac{dC}{dr} = 0 \text{ at } r = 0$$

and at outer surface

$$C = C_s \text{ at } r = r_s$$

Solve linear differential equation by conventional methods to yield

$$\frac{C}{C_s} = \frac{r_s \sinh\left(3\phi_s \frac{r}{r_s}\right)}{r \sinh 3\phi_s}$$

where ϕ_s is Thiele modulus for a spherical pellet defined by $\phi_s = \frac{r_s}{3}\sqrt{\frac{k_1\rho_s}{D_e}}$

Both D_e and k_1 are necessary to use $r_p = \eta k_1(C_A)_s$. D_e could be obtained from the reduced pore volume equation in case of no tortuosity factor.

$$D_e = (\varepsilon_s^2 D_{AB})$$

At 200°C , $D_e = (0.5)^2 (3.01\times10^{-5}) = 7.53\times10^{-6}$

At 250°C , $D_e = (0.5)^2 (3.62\times10^{-5}) = 9.04\times10^{-6}$

At 300°C , $D_e = (0.5)^2 (4.26\times10^{-5}) = 1.06\times10^{-5}$

Substitute radius of catalyst pellet , $r_s = 0.107\times10^{-3}$ m with ϕ_s equation

$$\phi_s = \frac{0.076\times10^{-3}\,\text{m}}{3}\sqrt{\frac{k(\text{m}^3/\text{s}-\text{kgcat.})\times1000(\text{kg/m}^3)}{1.06\times10^{-5}(\text{m}^2/\text{s})}}, \text{ at } 300^\circ\text{C}$$

$$\phi_s = 0.246\sqrt{k} \text{ (dimensionless)}$$

Find k from the mass balance equation around plug-flow reactor.

$$r_w = \frac{F_{Ao}dx}{dW}$$

where $r_w = kC_A$

Thus, $kC_A = \frac{F_{Ao}dx}{dW}$

$$kC_{Ao}(1\text{-}x) = \frac{F_{Ao}dx}{dW}$$

$$W = \frac{F_{Ao}}{kC_{Ao}}\int_0^{0.55}\frac{1}{1-x}dx$$

$$W = \frac{F_{Ao}}{kC_{Ao}}\left[-\ln(1-x)\right]_0 = \frac{F_{Ao}}{kC_{Ao}}(-\ln(0.45))$$

$$k = \frac{F_{Ao}}{WC_{Ao}}(-\ln(0.45))$$

$$k = \frac{2.65\times10^{-6}(\text{mol/s})}{0.1\times10^{-3}(\text{kg})\times1.03(\text{mol/m}^3)}(-\ln(0.45)) = 1.67\times10^{-2}\,\text{m}^3/\text{s - kg catalyst}$$

Calculate ϕ_s: $\phi_s = 0.246\sqrt{2.05\times10^{-2}} = 3.53\times10^{-2}$

At 200°C, conversion (x) = 0.20, k = 0.00037m^3/ s-kg catalyst, $\phi_s = 1.50 \times 10^{-2}$

At 250°C, conversion (x) = 0.39, k = 0.00820m^3/ s-kg catalyst, $\phi_s = 2.23 \times 10^{-2}$

At 300°C, conversion (x) = 0.55, k = 0.00167m^3/ s-kg catalyst, $\phi_s = 3.28 \times 10^{-2}$

For such small values of ϕ_s it was concluded that the internal mass transport has no effect on the rate of 1-propanol oxidation reaction.

APPENDIX C

CALIBRATION CURVE

Flame ionization detector gas chromatographs, model 14A and 14B, were used to analyze the concentrations of oxygenated compounds and light hydrocarbons, respectively, 1-propanol, propanal and formaldehyde were analyzed by GC model 14A while methane, ethene, propane and propene were analyzed by GC model 14B.

Gas chromatograph with the thermal conductivity detector, model 8A was used to analyze the concentrations of CO_2 and CO by using Porapak QS and Molecular Sieve 5A column, respectively.

The calibration curves of methane, ethene, propane, propene, 1-propanol, formaldehyde, propanal, CO and CO_2 are illustrated in the following figures.

Calibration curve

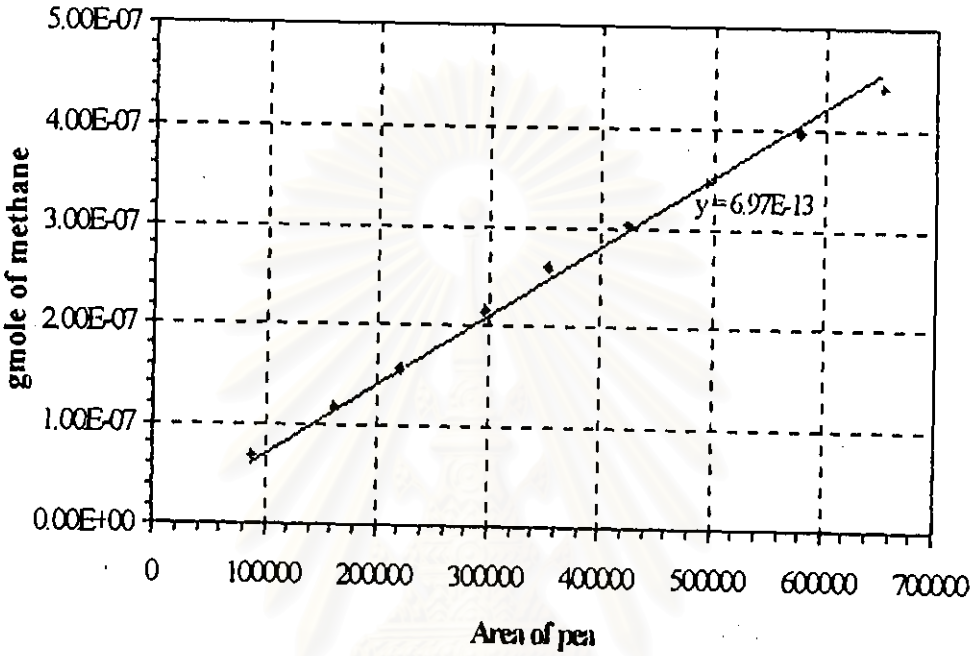

Figure C1 The calibration curve of methane

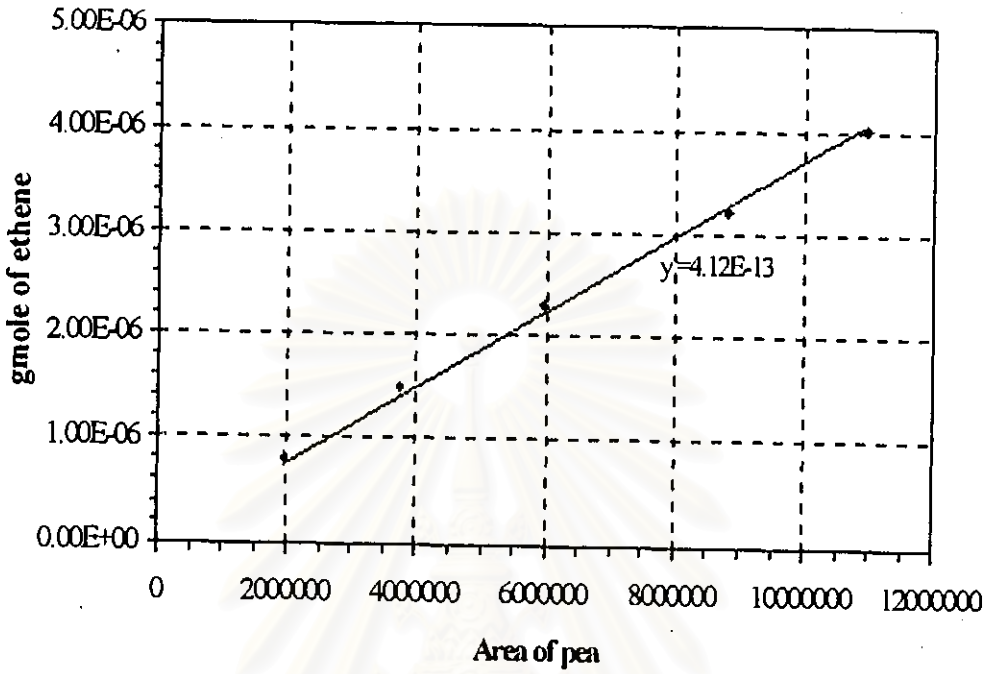

FigureC2 The calibration curve of ethene

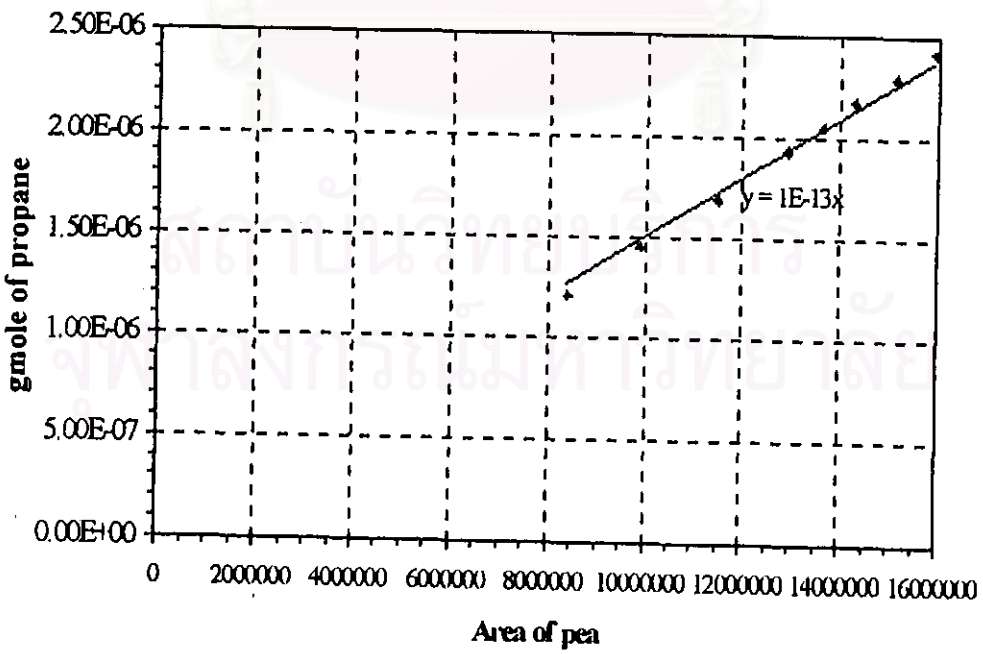

Figure C3 The calibration curve of propane

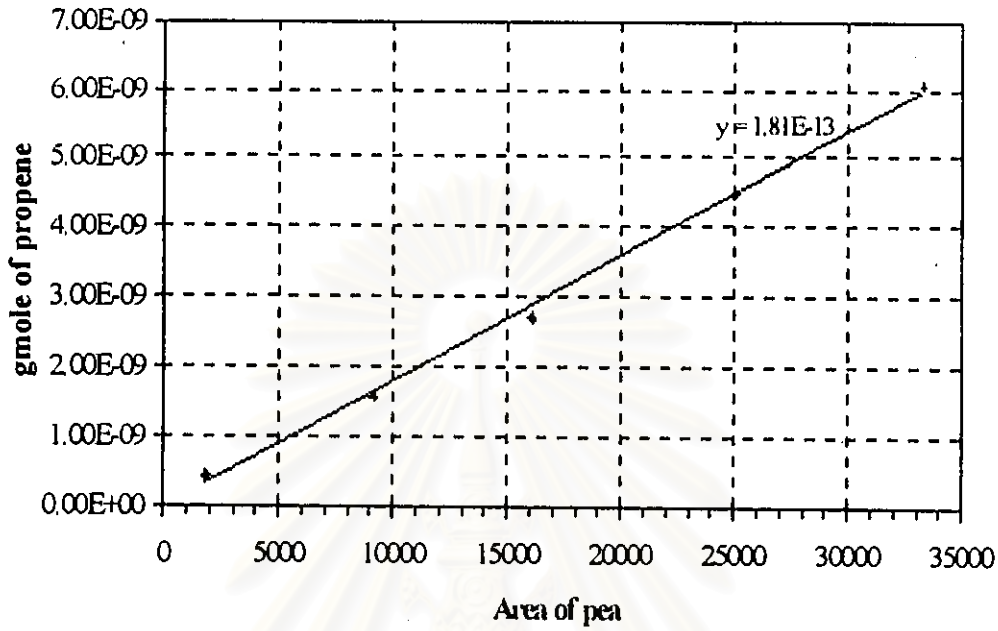

Figure C4 The calibration curve of propene

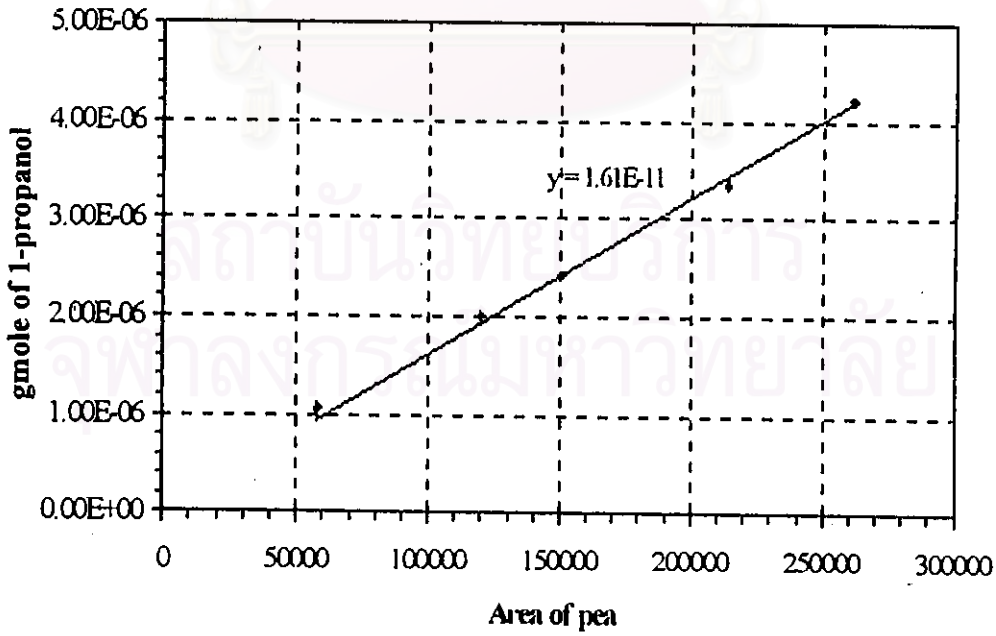

Figure C5 The calibration curve of 1-propanol

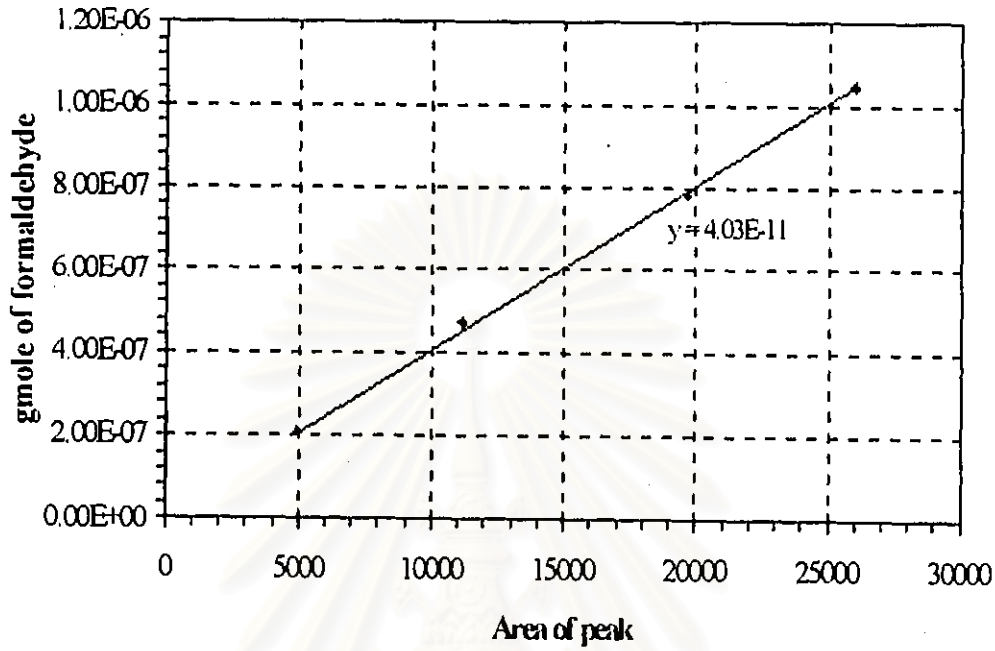

Figure C6 The calibration curve of formaldehyde

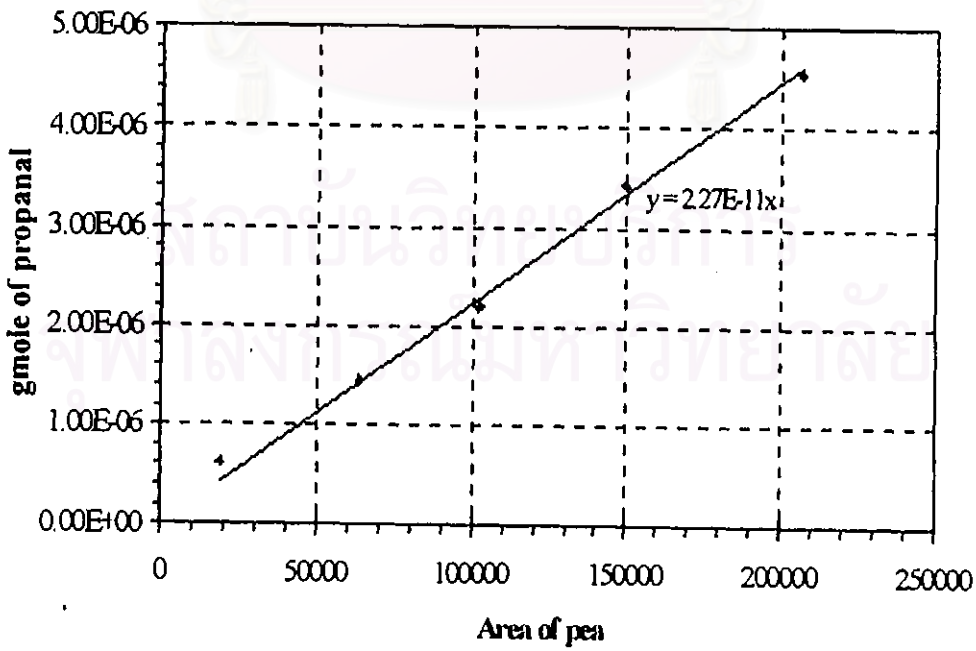

Figure C7 The calibration curve of propanal

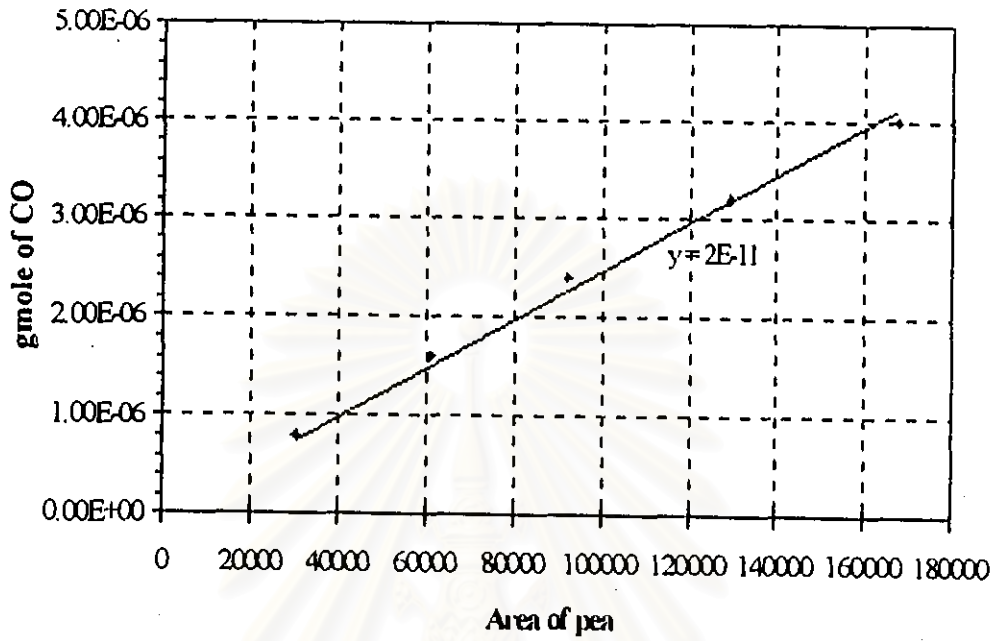

Figure C8 The calibration curve of CO

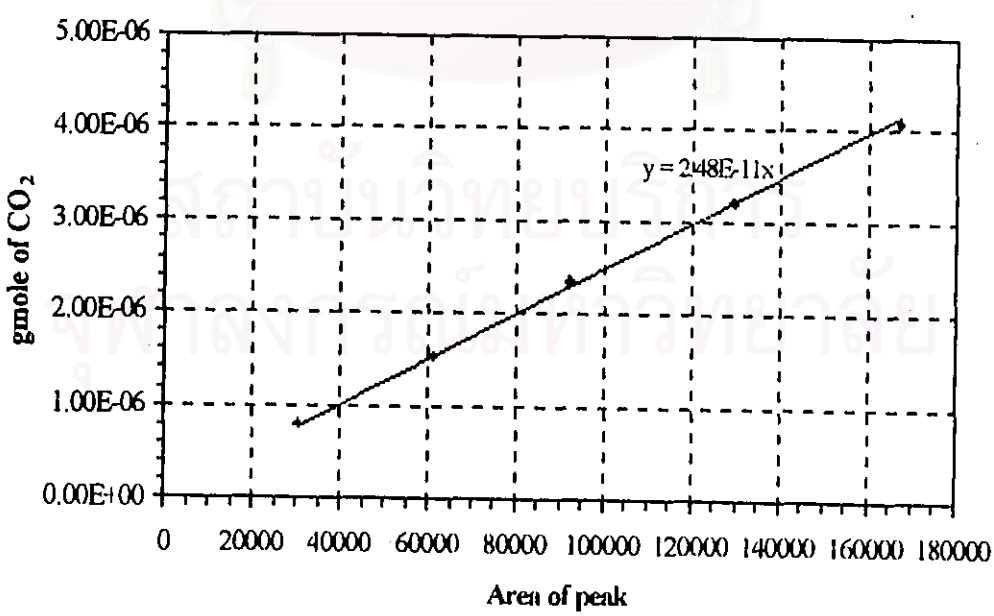

Figure C9 The calibration curve of CO_2

APPENDIX D
DATA OF EXPERIMENTS AND SAMPLE OF CHROMATOGRAM

Appendix D is divided in two part:

1. data of TPR experiment and the oxidation reaction
2. Chromatogram of hydrocarbon, CO, and CO_2

1) data of TPR experiment and the oxidation reaction

In this section, data of TPR experiment and the oxidation reaction are listed as below

D1 Data of TPR experiment

Table D1 Data of figure 5.9

Temp (°C)	H_2 (au)	Temp (°C)	H_2 (au)	Temp (°C)	H_2 (au)	Temp (°C)	H_2 (au)
50	130	220	725	390	1300	560	2850
60	190	230	760	400	1325	570	2920
70	240	240	810	410	1345	580	2875
80	290	250	830	420	1380	590	2845
90	375	260	870	430	1400	600	2810
100	415	270	900	440	1425	610	2700
110	450	280	945	450	1436	620	2610
120	470	290	985	460	1650	630	2500
130	490	300	1010	470	1790	640	2475
140	520	310	1034	480	1950	650	2465
150	550	320	1065	490	2100	660	2425
160	580	330	1099	500	2385	670	2400
170	600	340	1120	510	2490	680	2375
180	630	350	1185	520	2590	690	2345
190	655	360	1215	530	2600	700	2300
200	685	370	1245	540	2700		
210	700	380	1270	550	2775		

Table D2 Data of figure 5.10

Temp (°C)	H_2 (au)	Temp (°C)	H_2 (au)	Temp (°C)	H_2 (au)	Temp (°C)	H_2 (au)
50	130	220	725	390	1300	560	2850
60	190	230	760	400	1325	570	2920
70	240	240	810	410	1345	580	2875
80	290	250	830	420	1380	590	2845
90	375	260	870	430	1400	600	2810
100	415	270	900	440	1425	610	2700
110	450	280	945	450	1436	620	2610
120	470	290	985	460	1650	630	2500
130	490	300	1010	470	1790	640	2475
140	520	310	1034	480	1950	650	2465
150	550	320	1065	490	2100	660	2425
160	580	330	1099	500	2385	670	2400
170	600	340	1120	510	2490	680	2375
180	630	350	1185	520	2590	690	2345
190	655	360	1215	530	2600	700	2300
200	685	370	1245	540	2700		
210	700	380	1270	550	2775		

Table D3 Data of figure 5.11

Temp (°C)	H_2 (au)	Temp (°C)	H_2 (au)	Temp (°C)	H_2 (au)	Temp (°C)	H_2 (au)
50	133	220	780	390	2260	560	4520
60	192	230	826	400	2350	570	4620
70	236	240	863	410	2440	580	4700
80	271	250	920	420	2528	590	4820
90	306	260	973	430	2618	600	5000
100	338	270	1064	440	2730	610	5070
110	372	280	1163	450	2800	620	5130
120	404	290	1255	460	2950	630	5200
130	440	300	1327	470	3200	640	5240
140	467	310	1370	480	3300	650	5290
150	501	320	1430	490	3420	660	5350
160	547	330	1505	500	3600	670	5410
170	588	340	1623	510	3800	680	5460
180	630	350	1760	520	3940	690	5500
190	666	360	1900	530	4150	700	5540
200	704	370	2030	540	4320		
210	745	380	2150	550	4420		

D2 The data of oxidation reaction test

- *Propane oxidation*

Table D11 Data of figure 5.16

Temp (°C)	% Propane (C)	% CO_2 (S)	% Methane (S)	% Ethene (S)	%Propene (S)	% Olefin yield
300	0.00	0				
400	0.08	99				
425	0.76	100				
450	1.52	100				
475	2.00	99				
500	5.00	99				

Table D12 Data of figure 5.17

Temp (°C)	% Propane (C)	% CO2 (S)	% Methane (S)	% Ethene (S)	% Propene (S)	% Olefin yield
300	0					
325	0					
350	1	100				
375	4	100				
400	7	100				
425	50	70	4	30	8	19
450	57	65	4	32	9	23
475	65	60	4	32	10	27
500	70	55	6	34	11	31

Table D13 Data of figure 5.18

Temp (°C)	% Propane (C)	% CO_2 (S)	% Methane (S)	% Ethene (S)	% Propene (S)	% Olefin yield
300						
350	3	100				
375	5	100				
400	26	98	0	0	1	0
425	80	90	0	5	1	5
450	89	85	1	9	2	10
475	92	85	0	6	1	7
500	93	85	1	8	1	9

- *1-Propanol oxidation*

Table D14 Data of figure 5.19

Temp (°C)	1-Propanol (C)	CO_2 (S)	Propanal (S)	Ethene (S)	Formaldehyde (S)
100	1	0	100		
150	2	0	100		
200	5	1	100		0
250	10	3	95		3
300	42	38	0		6
350	71	55	0		8
400	94	70	0	0	2
450	98	82	0	20	39
500	99	95	0	0	20

Table D15 Data of figure 5.20

Temp (°C)	1-Propanol (C)	CO_2 (S)	Propanal (S)	Ethene (S)	Formaldehyde (S)
100	1		100		
150	3	3	100		
200	19	8	85	3	
250	38	16	7	5	2
300	55	52	0	8	10
350	80	68	0	18	3
400	95	86	0	6	0
450	100	95	0	0	0
500	100	100	0	0	0

Table D16 Data of figure 5.21

Temp (°C)	1-Propanol (C)	CO_2 (S)	Propanal (S)	Ethene (S)	Formaldehyde (S)
100	1	0	100		
150	2	0	100	0	0
200	3	7	80	5	8
250	40	50	30	0	12
300	75	70	10	0	0
350	98	90	0	0	0
400	100	95	0	0	0
450	100	100	0	0	0
500	100	100	0	0	0

Table D17 Data of figure 5.22

Temp (°C)	1-Propanol (C)	CO_2 (S)	Propanal (S)	Ethene (S)	Formaldehyde (S)
100	0	1	100		0
150	3	2	100		5
200	12	10	80		22
250	45	57	0	0	13
300	85	77	0	0	8
350	100	98	0	0	0
400	100	99	0	0	0
450	100	100	0	0	0
500	100	100	0	0	0

- *Propene oxidation*

Table D18 Data of figure 5.28

Temp (°C)	Propene (C)	CO_2 (S)
100	0	
150	0	
200	0	
250	0	
300	3	100
350	75	99
400	79	100
450	88	99
500	100	100

- *CO oxidation*

Table D19 Data of figure 5.29

Temp (°C)	CO (C)	CO_2 (S)
100	0	
150	4	100
200	30	99
250	80	100
300	100	99
350	100	100
400	100	99
450	100	100
500	100	100

Sample of chromatogram

In this section the chromatogram of reactant and reaction product are shows below:

2.1 Chromatogram of methane, ethene, propane, and propene

The low molecular weight hydrocarbons such as methane, ethene, paopane, and propene are detected by Gas Chromatograph GC 14B. The chromatogram of each hydrocarbon occur at different time as show in figure D1

Methane : 0.97 min
Ethene : 3.45 min.
Propane : 8.02 min
Propene : 14.2 min.

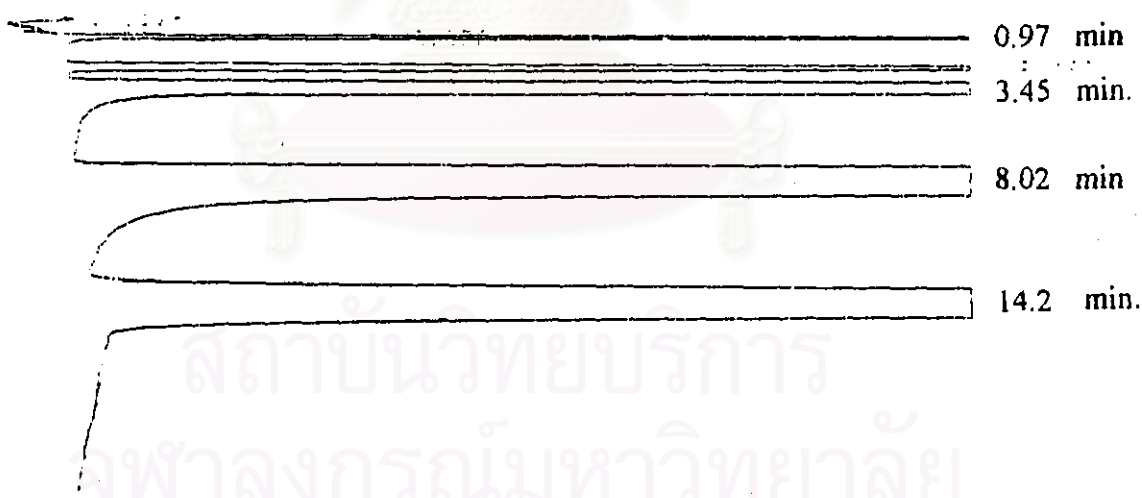

Figure D1 The chromatogram of hydrocarbons.

2.2 Chromatogram of 1- propanol, propanal, and formaldehyde

The Chromatogram of oxygenate compounds such as 1-propanol, propanal, and formaldehyde detected by Gas Chromatograph GC 14A are showed in figure D2 below.

Formaldehyde :		4.06	min.
Propanal	:	4.54	min.
1-Propanol	:	5.52	min.

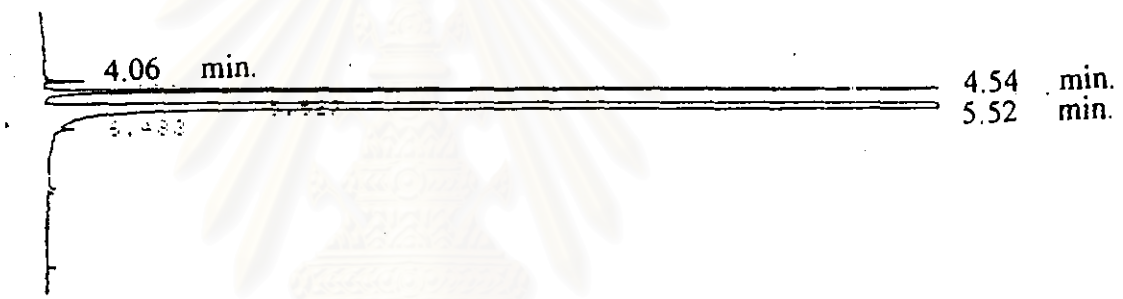

Figure D2 The chromatogram of oxygenate compounds.

2.3 Chromatogram of CO and CO_2

Air, CO, and CO_2 are detected by Gas Chromatograph GC 8A. The chromatogram of air, CO and CO_2 are demonstrated in figure D3 below.

Air : 0.78 min. (Porapak-Q column)
CO_2 : 1.74 min. (Porapak-Q column)
CO : 14.51 min. (MS-5A)

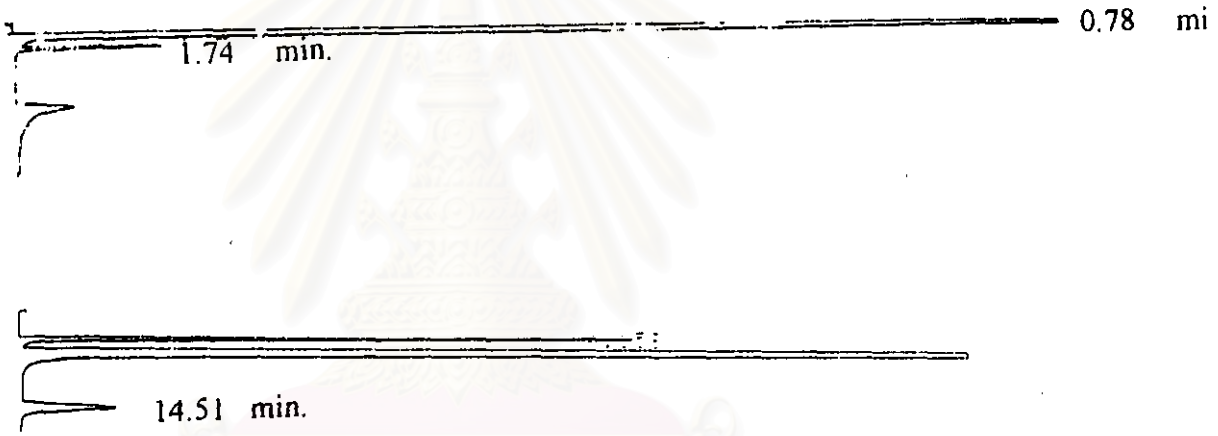

Figure D3. Chromatogram of air, CO and CO_2

APPENDIX E

PUBLISHED PAPER

This published paper emerged during this study was presented at Academic Conference, 8th, Mahidol University, 17-18 December, 1998.

ผลของตัวรองรับที่มีต่อคุณสมบัติในการออกซิเดชันของโคบอลต์ออกไซด์

นางสาววนิดา ยังวนิชเศรษฐ, ผศ.ดร.ธราธร มงคลศรี*

ภาควิชาวิศวกรรมเคมี คณะวิศวกรรมศาสตร์

จุฬาลงกรณ์มหาวิทยาลัย กรุงเทพฯ 10330

บทคัดย่อ

ได้ทำการศึกษาตัวเร่งปฏิกิริยาโคบอลต์ออกไซด์บนตัวรองรับ 3 ชนิด คือ แกมมา-อลูมินา (γ-Al_2O_3), แมกเนเซียมออกไซด์ (MgO) และ ไททาเนีย (TiO_2 anatase) โดยใช้ปฏิกิริยาออกซิเดชันของโพรเพน จากการทดลองพบว่าตัวเร่งปฏิกิริยาที่เตรียมขึ้น จะมีความว่องไวในการทำปฏิกิริยาในช่วงอุณหภูมิ 200-500°C โดยความว่องไวในการทำปฏิกิริยาออกซิเดชันของโคบอลต์ออกไซด์บนตัวรองรับ จะเรียงลำดับดังนี้ : γ-Al_2O_3 > MgO > TiO_2 (anatase) จากการทดลองยังพบว่า ตัวรองรับยังส่งผลต่อค่าการเลือกเกิดผลิตภัณฑ์ได้ โดย Co_3O_4/γ-Al_2O_3 จะให้ผลิตภัณฑ์หลักเป็น CO_2, CO, CH_4, C_2H_4 และ C_3H_6 ส่วน Co_3O_4/MgO จะให้ผลิตภัณฑ์เป็น CO_2, CH_4, C_2H_4 และ C_3H_6และ Co_3O_4/TiO_2 จะให้ผลิตภัณฑ์เป็น CO_2 และ C_3H_6 และพบว่าตัวเร่งปฏิกิริยา 8%Co_3O_4/MgO จะให้โอเลฟินส์ยีลด์สูงสุดประมาณ 35 % ที่อุณหภูมิ 500 °C

Effect of supports on the oxidation property of cobalt oxide

Wanida Youngwanishsate, Tharathon Mongkhonsi*
Petrochemical Engineering Laboratory, Department of Chemical Engineering,
Chulalongkorn University, Bangkok 10330 Thailand.
*To whom correspondance be addressed

Abstract

Propane oxidation has been performed on cobalt oxide supported on γ-Al_2O_3, MgO and TiO_2 (anatase). The supported cobalt oxide has been found active for propane oxidation at temperature 200-500 °C. From the experiment the catalytic activity for propane oxidation of the cobalt species on different supports decreases in the order : γ-Al_2O_3 > MgO > TiO_2 (anatase) and the product selectivity depend on the nature of support. The products from 8%Co_3O_4/γ-Al_2O_3 are CO_2, CO, CH_4, C_2H_4 and C_3H_6, 8%Co_3O_4/MgO are CO_2, CH_4, C_2H_4 and C_3H_6 and 8%Co_3O_4/TiO_2 (anatase) are CO_2 and C_3H_6. The highest olefin yields of ca. 35% at 500 °C has been obtained for 8%Co_3O_4/MgO catalyst.

Keywords: Cobalt oxide, Magnesium oxide, Titania; propane oxidation

1. Introduction

Oxidation of organic vapor in the presence of solid catalysts has gained importance as one of the promising methods for organic synthesis and air pollution control. To develop new transition-metal based catalytic materials, knowledge of the reaction is desirable. In the cases of the selective oxidation reactions over metal oxide catalysts the so-called Mars-van Krevelen or redox mechanism has been widely accepted, where the oxidized catalyst surface oxidizes the reactant, and is reoxidized by gas-phase O_2 in a separate step. The active oxygen species in selective oxidation are generally assumed to be lattice oxide O^{2-} species [1]. For the oxidative dehydrogenation of propane to propylene over magnesium molybdate catalysts, the lattice oxide ions of catalyst surface acted as active oxygen species in the reaction [2].

Cobalt oxides have been interested materials in the field of heterogeneous catalysis and surface chemistry. Among the binary metal oxides Co_3O_4 showed the highest catalytic activity for the combustion of organic compounds [3]. Cobalt oxide supported on alumina catalysts actived for total oxidation of methane [4]. Sinha and Shankar have investigated that total oxidation of n-hexane, presented in lean mixtures, was carried out on cobalt oxide catalysts supported on silica gel and found that the activity of several catalysts depended on their method of preparation [5]. Okamoto et.al found that cobalt oxide supported on Al_2O_3 catalysts prepared from cobalt acetate show higher cobalt dispersion than catalysts prepared from cobalt nitrate [6]. Co_3O_4 has been found more active than $MgCr_2O_4$, CuO and Mn_3O_4 catalysts for propane oxidation. Mars-van Krevelen mechanism, impling lattice oxide ions as the active oxygen species, was likely to apply to both partial and total oxidation [7,8]. Grabowski et al. [9] have investigated that oxidation of butane over chromia supported on SiO_2, Al_2O_3, TiO_2, ZrO_2 and MgO. The total activity and selectivity to isobutene depending on the nature of the support.

In the present work, we have investigated effect of supports on the catalytic property of cobalt oxide supported on γ-Al_2O_3, MgO and TiO_2 (anatase). The catalysts were characterized by Atomic Absorption Spectroscopy (AAS), Fourier-transform Infrared (FT-IR) and X-ray powder diffraction (XRD). Catalytic activities of catalysts have been tested for oxidation of propane.

2. Experimental

2.1 Catalyst preparation

Cobalt oxide supported on γ-Al_2O_3, MgO and TiO_2 (anatase) were prepared, containing 8% of cobalt content .

8%Co_3O_4/γ-Al_2O_3 catalysts were prepared by impregnating γ-Al_2O_3 (mesh 40-60) with an aqueous solution of cobalt acetate ($Co(CH_3COO)_2 \cdot 4H_2O$). The amount of the aqueous solution was adjusted to be 0.5 cm^3 per gram of γ-Al_2O_3, left 6 h at room temperature. The solid were dried at 120 °C for 12 h, then calcined in air at 500 °C.

8%Co_3O_4/TiO_2 (anatase) and 8%Co_3O_4/ MgO were prepared by wet impregnation method, in which the catalyst slurry was evaporated to dryness at 70-80°C over a water bath with vigorous stirring. After the catalyst precursor had been dried at 120 °C for 12 h, it was calcined at 500 °C for 8%Co_3O_4/TiO_2 (anatase) and 600 °C for 8%Co_3O_4/MgO, respectively.

2.2 Characterization techniques

2.2.1 Atomic absorption spectroscopy (AAS)

Percentage of metal cobalt loading was measured by atomic absorption spectroscopy (AAS).

2.2.2 Powder X-ray diffraction (XRD)

The phase structures were determined by X-ray diffraction. A Siemens D 5000 X-ray diffractometer using Cu Kα filtered radiation in the range of 4-80 °.

2.2.3 Fourier transform Infrared (FT-IR)

The IR spectra of catalysts were determined by FT-IR using Nicolet model Impact 400.equipped with a TGS detector.

2.2 Catalytic activity tests

Propane oxidation reaction was performed in a continuous flow fixed-bed reactor equipped with a quartz-tubular reactor (9 mm. O.D.) at atmospheric pressure. The feed composition was 4 mol% of propane and 96 mol% of air in the temperature range of 200-500 °C.

Approximately, 0.1 g of catalyst was used and the temperature was measured with a thermocouple located just below the catalyst bed. The total flow-rate into the reactor was 100 ml/min.

CO_2 and CO were alternately analyzed on-line by a Shimadzu GC8A gas chromatograph equipped with a thermal conductivity detector, a 5A molecular sieve column for separating CO and a Polapak-Q column for CO_2. While hydrocarbons were analyzed by flame ionization detector gas chromatograph Shimadzu 14B.

3. Results and discussion

3.1 Catalyst characterization

The chemical composition and specific surface area of the catalysts are listed in table 1.

Table 1. List of the catalysts

Catalyst	Cobalt composition (wt%)
Co_3O_4/Al_2O_3	6.8
Co_3O_4/MgO	7.6
Co_3O_4/TiO_2 (anatase)	7.1

The X-ray diffraction patterns (fig.1) of supported catalysts show only the crystalline of support and IR spectra (fig.2) of supported catalysts show only absorption bands of supports probably because of their low concentration of cobalt oxide content .

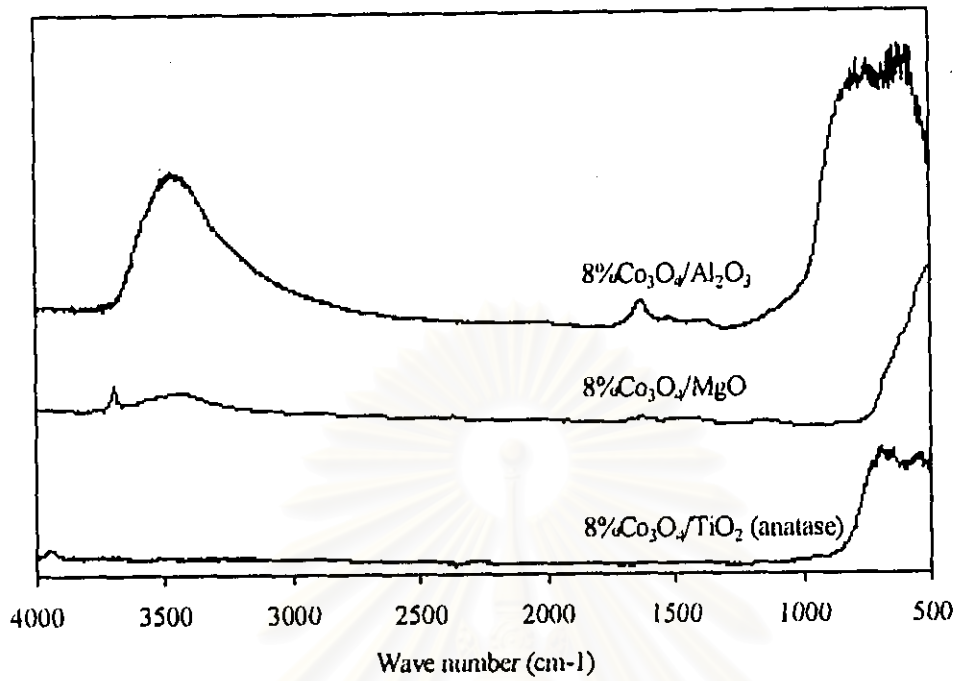

Fig. 1. FTIR spectra of supported cobalt oxide catalysts.

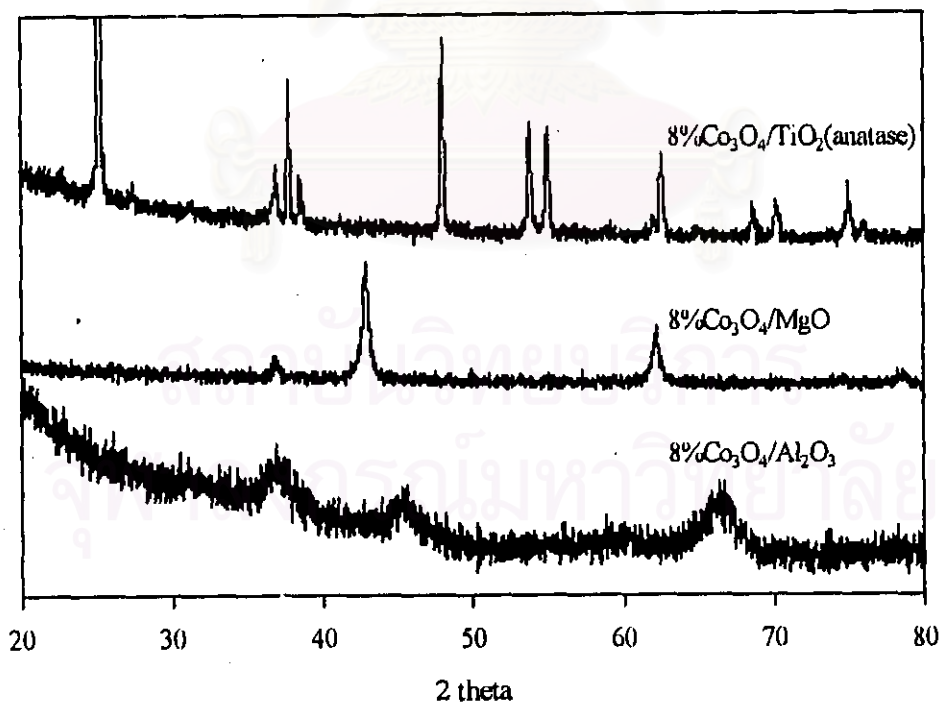

Fig. 2. X-ray diffraction pattens of supported cobalt oxide catalysts.

3.2 Propane oxidation

- *8%Co_3O_4/γ-Al_2O_3*

The behavior of 8%Co_3O_4/γ-Al_2O_3 as a catalyst for propane oxidation in C_3H_8 : Air mixtures is showed in fig. 3. The conversion of propane becomes measurable in the 200-500 °C range. The maximum propane conversion is ca.90 % at 500 °C.

The main products are CO and CO_2 with small amount of methane, ethylene and propylene as by products. During 350-500 °C the olefin yield remain constant ca. 17 %.

The sum of selectivities fulfils 100 % within uncertainty limits; showing that the carbon balance is actual fulfilled.

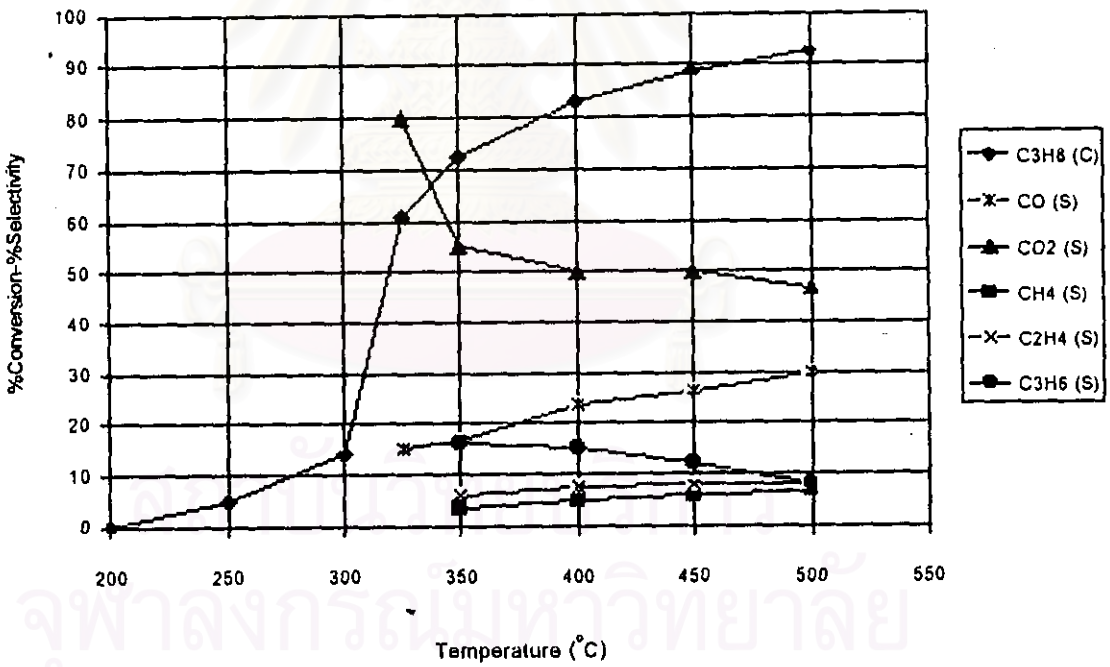

Fig.3. Conversion (C) of propane and product selectivities (S) on 8%Co_3O_4/γ-Al_2O_3.

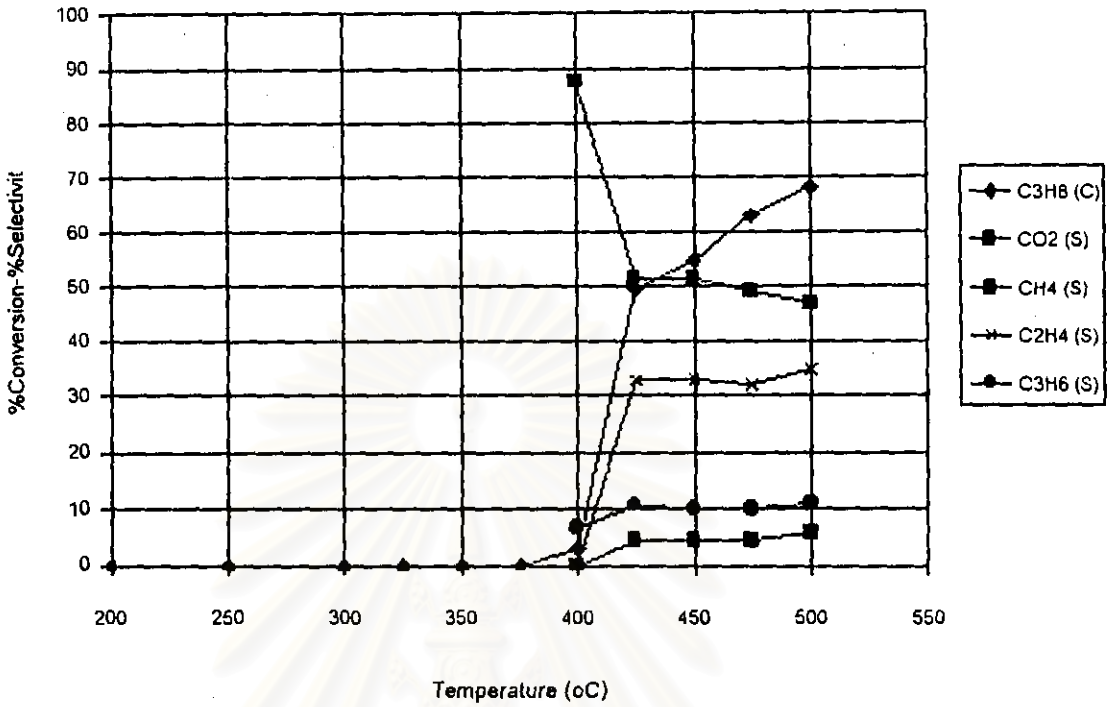

Fig. 4. Conversion (C) of propane and product selectivities (S) on 8%Co_3O_4/MgO.

- *Propane oxidation on 8%Co_3O_4/MgO*

From fig. 4 the conversion of propane over 8%Co_3O_4/MgO becomes detectable at 400 °C. The maximum propane conversion is ca. 70 % and the maximum olefin yield is ca. 32 % at 500 °C.

The main products are CO_2 and ethylene with methane and propylene are by products. No CO is measured among the products.

- *Propane oxidation on 8%Co_3O_4/TiO_2 (anatase)*

From fig. 5 conversion of propane becomes measurable at 250 °C. At 500 °C the maximum propane conversion is ca. 20 %. The highest selectivity to propylene is ca. 55 % at ca. 1% conversion at 250 °C.

The main product observed are CO_2 and propylene and small amounts of ethylene is detected.

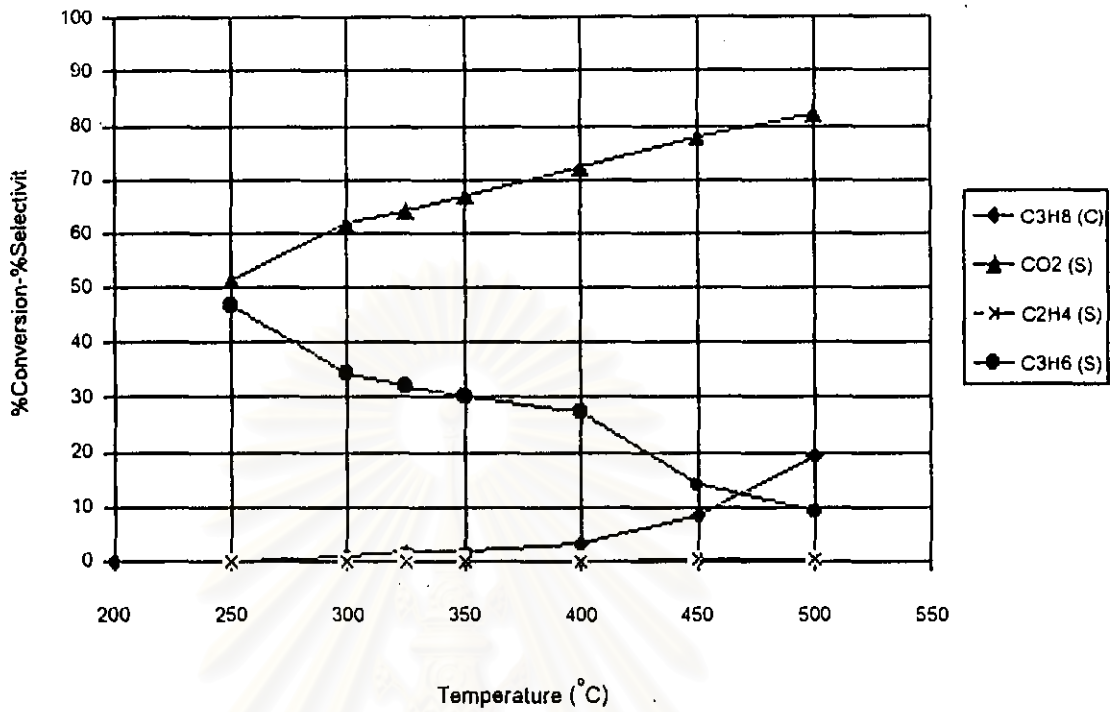

Fig. 5. Conversion (C) of propane and product selectivities (S) on 8% Co_3O_4/TiO_2.

From 8%Co_3O_4/γ-Al_2O_3 when the propane conversion increase, the selectivity to propylene decrease. In contrast the selectivity to CO increase. Such a behavior for propane oxidation reaction may be due to the mechanism of the formation of CO from the intermediate product-propylene. On the other hand, for CO_2, methane and ethylene form in parallel route with the formation of propylene.

8%Co_3O_4/MgO during 400-425 °C the CO_2 selectivity decreases significantly whereas the methane. ethylene and propylene selectivities increase. After 425 °C all product selectivities remain constant. From these data allow us to propose tentatively the pathway that all products form in parallel route.

8%Co_3O_4/TiO_2 (anatase) propylene selectivity decreases and CO_2 selectivity increases with increasing propane conversion. Such a behavior may be due to the consecutive mechanism of the formation of CO_2 from the intermediate product-propylene.

4. Conclusions

The conclusion from the present study are the following.

(1). Catalytic performance of supported cobalt oxide depend on the nature of the support. The catalytic activity for propane oxidation of the cobalt species on different supports decreases in the order: γ-Al_2O_3 > MgO > TiO_2 (anatase).

(2). Product selectivity from propane oxidation are different depending on the type of support.

(3). The highest olefin yield ca. 35 % have been found for 8%Co_3O_4/MgO.

Acknowledgement

The authors would like to thank Thailand Research Fund (TRF) for financial support and Prof. Piyasan Praserthdam for his helpful suggestion.

References

1. E. Finocchio, G. Busca, V. Lorenzelli and V. S. Escribano. "FTIR studies on the selective oxidation and combustion of light hydrocarbons at metal oxide surfaces Part 2". *J. Chem. Soc., Faraday Trans.*, 1996, **92**(9), 1587-1593 .
2. Y. S. Yoon, W. Ueda and Y. Moro-oka. " Oxidative dehydrogenation of propane over magnesium molybdate catalysts". *Catal. Lett.*, 1995, **35**, 57-64.
3. G. Busca, R. Guidetti and V. lorenzelli. "Fourier-transform Infrared Study of the Surface Properties of Cobalt Oxides". *J. Chem. Soc., Faraday Trans.*, 1990, **86**(6), 989-994 .
4. E. Garbowski, M. Guenin, M-C. Marion and M. Primet. "Catalytic Properties and Surface States of Cobalt Containing Oxidation Catalysts". *Appl.Catal.*, 1990, **64**, 209-224.
5. A. S. K. Sinha and V. Shankar. "Low-Temperature Catalysts for Total Oxidation of n-Hexane". *Ind. Eng. Chem. Res.*, 1993, **32**, 1061-1065.

6. Y. Okamoto, T. Adachi, K. Nagata, M. Odawara and T. Imanaka. "Effects of starting cobalt salt upon the cobalt-alumina interactions and hydrodesulfurization activity of CoO/Al_2O_3". *Appl. Catal.*, 1991, **73**, 249-265.
7. E. Finocchio, R. J. Willey, G. Busca and V. Lorenzelli. "FTIR studies on the selective oxidation and combustion of light hydrocarbons at metal oxide surfaces Part 3". *J. Chem. Soc., Faraday Trans.*, 1997, **93**(1), 175-180.
8. M. Baldi, E. Finocchio, F. Milella and G. Busca. "Catalytic combustion of C3 hydrocarbons and oxygenates over Mn_3O_4". *Appl. Catal.*, 1998, **16**, 43-51.
9. R. Grabowski, B. Grzybowska, J. Sloczynski and K. Wcislo. Oxidative dehydrogenation of isobutane on supported chromia catalysys".*Appl.Catal.*,1996, **144**, 335-341.

VITA

Miss Wanida Youngwanisgsate was born in Choomporn on February 21, 1974. She received her bachelor of engineering degree of chemical engineering from Chulalongkorn University in 1996.